Supplementary Information

Engineered FGF19 reduces liver injury and resolves sclerosing cholangitis in *Mdr2*-deficient mice

Mei Zhou, R. Marc Learned, Stephen Rossi, Alex M. DePaoli, Hui Tian and Lei Ling*

NGM Biopharmaceuticals, Inc., 630 Gateway Blvd., South San Francisco, CA 94080, USA

*Correspondence: lling@ngmbio.com

Supplementary Materials and Methods

Supplementary Figure 1

Supplementary Figure 2

Supplementary Figure 3

Supplementary Figure 4

SUPPLEMENTARY EXPERIMENTAL PROCEDURES

Animals and animal care. Mice were housed in a pathogen-free animal facility at 22ºC under controlled 12 hour light/12 hour dark cycle, kept on standard chow diet (Teklad 2918), and autoclaved water ad libitum. All *in vivo* studies were conducted in 2-3 independent experimental animal cohorts. Sample sizes were determined on the basis of homogeneity and consistency of characteristics in the selected models and were sufficient to detect statistically significant differences in chemistry parameters between groups. Mice were randomized into the treatment groups based on body weight. The investigators were blinded during group allocation but not blinded during *in vivo* characterization. 12 week-old *Mdr2*-/- mice (males and females) received a single intravenous dose of $1x10^{11}$ v.g. of AAV containing either FGF19, M70, or a control gene green fluorescent protein. Blood concentrations of liver enzymes, lipids and total bile acids were determined before, 4 and 24 weeks after AAV injection. Mice were euthanized 24 weeks post AAV administration and examined for histology and gene expression analysis. Female Mdr2-/- mice were used for the 32-week hepatocarcinogenicity study. All injections and tests were performed during the light cycle. No samples or animals were excluded from the *in vivo* pharmacological analysis.

Histology. Upon study termination, livers were removed after macroscopic examination and liver weight recording, fixed in 10% neutral-buffered formalin and embedded in paraffin. Sections (4 μm thick) were subjected to standard H&E, Sirius red or trichrome staining. For immunohistochemical studies, tissue sections were stained with antibodies against glutamine synthetase (Thermo Fisher) for liver tumor evaluation. Additionally, slides were incubated with anti-Ki-67 (Dako) to assess proliferation, or anti-α-SMA (Sigma) to characterize myofibroblasts. Biotinylated secondary antibodies, ABC-HRP reagent and DAB colorimetric peroxidase

substrate (Vector Laboratories), were used for detection. For bile duct staining with *Dolichos biflorus* agglutinin-fluorescein (Vector Laboratories), sections were mounted in media containing 4,6-diamidino-2-phenylindole (DAPI) (Sigma) for nuclear visualization. Digital imaging microscopy was performed using a Leica DM4000 microscope equipped with DFC500 camera and a scanning platform (Leica) and morphometrically quantified using ImagePro (Media Cybernetics) and ImageJ (NIH) softwares.

Gallbladder volume, composition and gallstone characteristics. 12 weeks after AAV-mediated transgene expression, female *Mdr2*-/- mice or wild type mice were fasted overnight but allowed free access to water. After cholecystectomy, gallbladder volume was determined by weighing the whole gallbladder, assuming a density of 1g/ml bile. Gallstones were counted under a headband magnifier and the maximum sizes of the gallstones were recorded. Phospholipid concentrations in the gallbladder bile were measured enzymatically using phospholipase D and choline oxidase with a colorimetric kit from Cayman Chemicals. Concentrations of total bile acids in gallbladder bile were determined using a 3α-hydroxysteroid dehydrogenase method (Diazyme).

DNA constructs. Human FGF19 (NM_005117) cDNA was cloned in-house. Mutations were introduced in the FGF19 constructs using the QuickChange Site-Directed Mutagenesis kit (Stratagene).

AAV production. AAV293 cells (Agilent Technologies) were cultured in Dulbeco's Modification of Eagle's Medium (DMEM; Mediatech) supplemented with 10% fetal bovine serum and 1x antibiotic-antimycotic solution (Mediatech). The cells were transfected with 3 plasmids (AAV transgene, pHelper (Agilent Technologies) and AAV2/9) for viral production.

EF1α promoter was used to drive transgene expression. Viral particles were purified using a discontinued iodixanal (Sigma) gradient and re-suspended in phosphate-buffered saline (PBS) with 10% glycerol and stored at –80ºC. Viral titer or vector genome number was determined by quantitative PCR.

Gene expression analysis. Total RNA was isolated from livers from female *Mdr2*-/- mice and wild type mice using the RNeasy kit (Qiagen). Real-time quantitative PCR assays were performed using QuantiTect multiplex qRT-PCR master mix (Qiagen) and premade primers and probes (Life Technologies) on Applied Biosystems 7900HT Sequence Detection System. Relative mRNA levels were calculated by the comparative threshold cycle method using GAPDH as the internal standard.

Statistics. All results are expressed as mean $\pm$ SEM. One-way ANOVA followed by Dunnett's post-test was used to compare data from multiple groups (GraphPad Prism). When indicated, unpaired, two-tailed Student's *t*-test was used to compare two treatment groups. For evaluating changes in liver enzymes over time, two-way ANOVA followed by Sidak's post-test (GraphPad Prism) was used for statistical analysis. A *P* value of 0.05 or less was considered statistically significant.

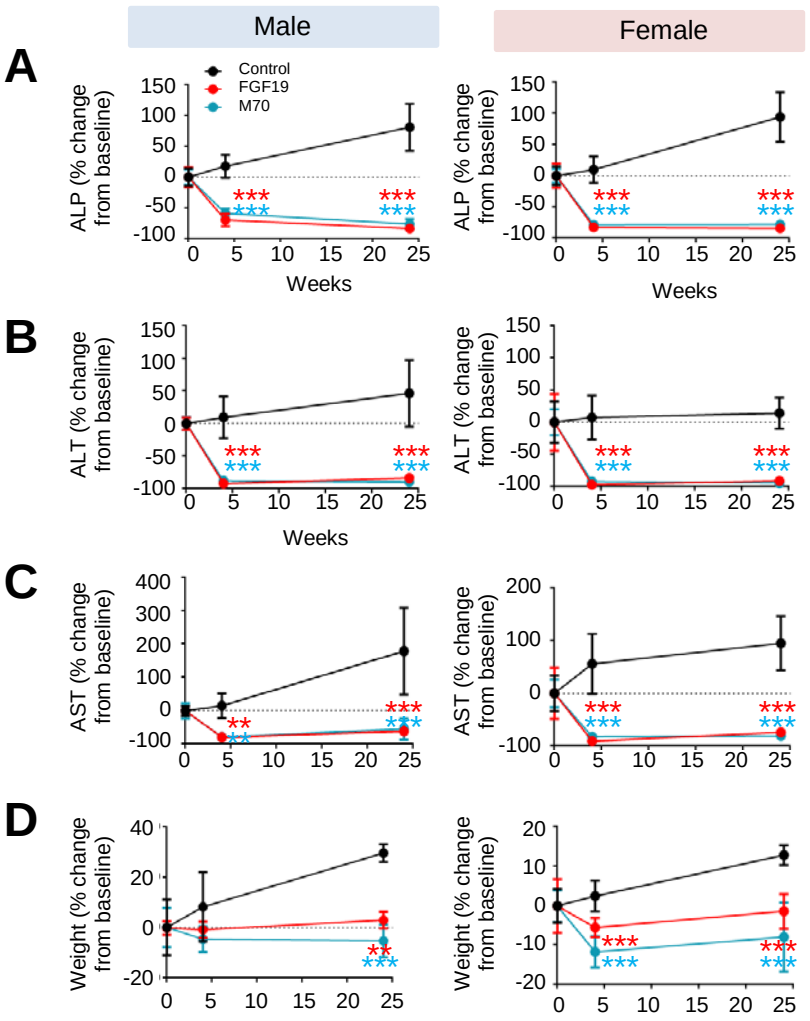

Supplementary Figure 1. FGF19 and M70 markedly reduce serum levels of liver enzymes in *Mdr2*-/- mice. 12-week old *Mdr2*-/- mice were injected with AAV carrying FGF19, M70, or a control gene GFP (n = 5 per sex per group). Liver enzymes were determined before, 4 and 24 weeks after AAV administration. (**A**) Percent changes from baseline in serum levels of alkaline phosphatase (ALP) over time (n = 5). Dashed line indicates baseline. (**B**) Percent changes from baseline in serum levels of alanine aminotransferase (ALT) over time (n = 5). Dashed line indicates baseline. (**C**) Percent changes from baseline in serum levels of aspartate aminotransferase (AST) over time (n = 5). Dashed line indicates baseline. (**D**) Percent changes from baseline in body weight over time (n = 5). Values are mean ± SEM. ***P < 0.001, **P < 0.01 versus control group by two-way ANOVA.

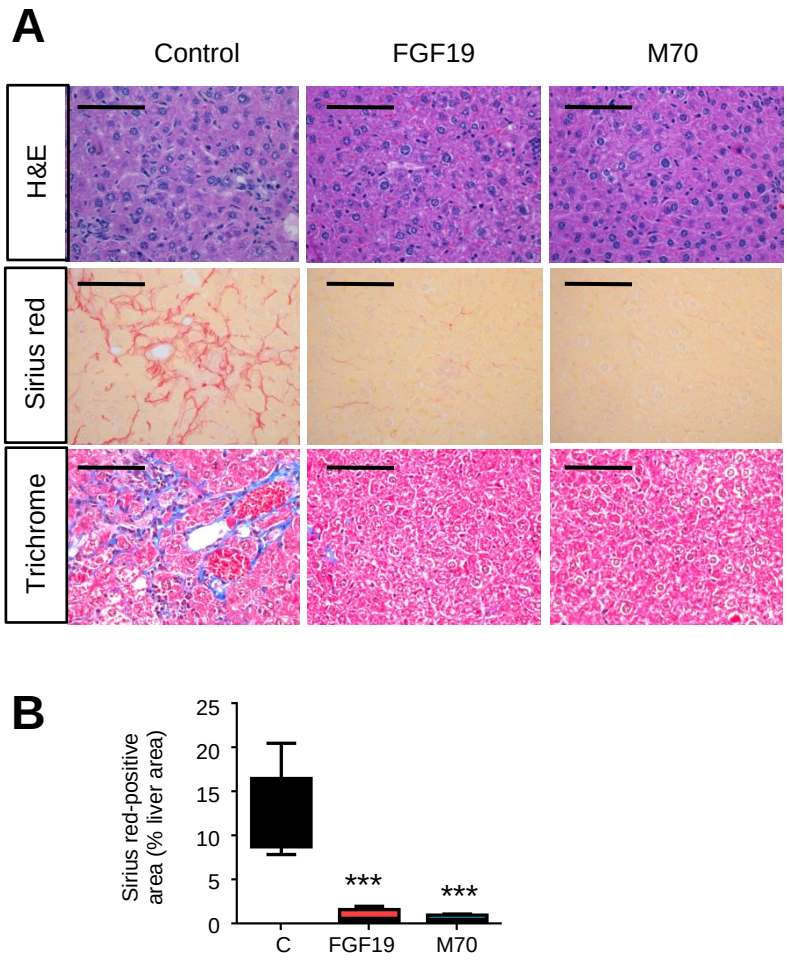

Supplementary Figure 2. FGF19 and M70 reduce hepatocellular fibrosis in *Mdr2*-/- mice. 12-week old *Mdr2*-/- mice were injected with AAV carrying FGF19, M70, or a control (C) gene (n = 5 per group). Hepatocellular fibrosis was assessed 24 weeks after AAV administration. **(A)** Representative images of liver stained with H&E, Sirius red, or trichrome. Livers from *Mdr2*-/- mice treated with control virus are fibrotic which appear red in Sirius red staining, and blue in trichrome staining. Scale bars, 100 μm. (B) Morphometric quantification of hepatocellular fibrosis. Sirius red-positive areas as percentage of total area were quantified using ImageJ program. Values are mean ± SEM. ***P < 0.001 versus control group by one-way ANOVA.

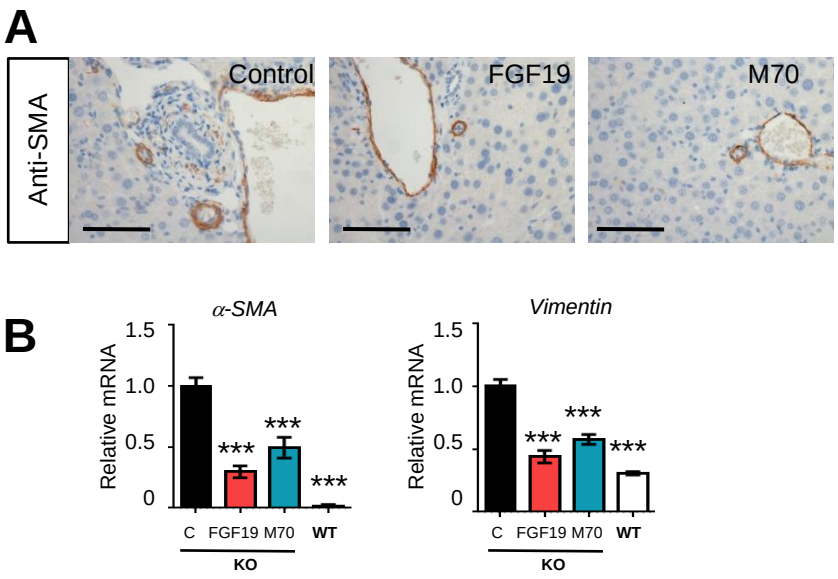

Supplementary Figure 3. FGF19 and M70 reduce markers of myofibroblasts in *Mdr2*-/- mice. 12-week old *Mdr2*-/- mice were injected with AAV carrying FGF19, M70, or a control (C) gene (n = 5 per group). Livers were assessed 24 weeks after AAV administration. (**A**) Representative images of liver stained with anti-α-smooth muscle actin (α-SMA). α-SMA is stained brown from DAB substrates. Scale bars, 100 μm. (**B**) mRNA levels of markers of myofibroblasts (n = 5). *Mdr2*+/+ mice (WT) were included as comparators for *Mdr2*-/- mice (KO) in gene expression analysis. Values are mean + SEM. ***P < 0.001 versus control group by one-way ANOVA.

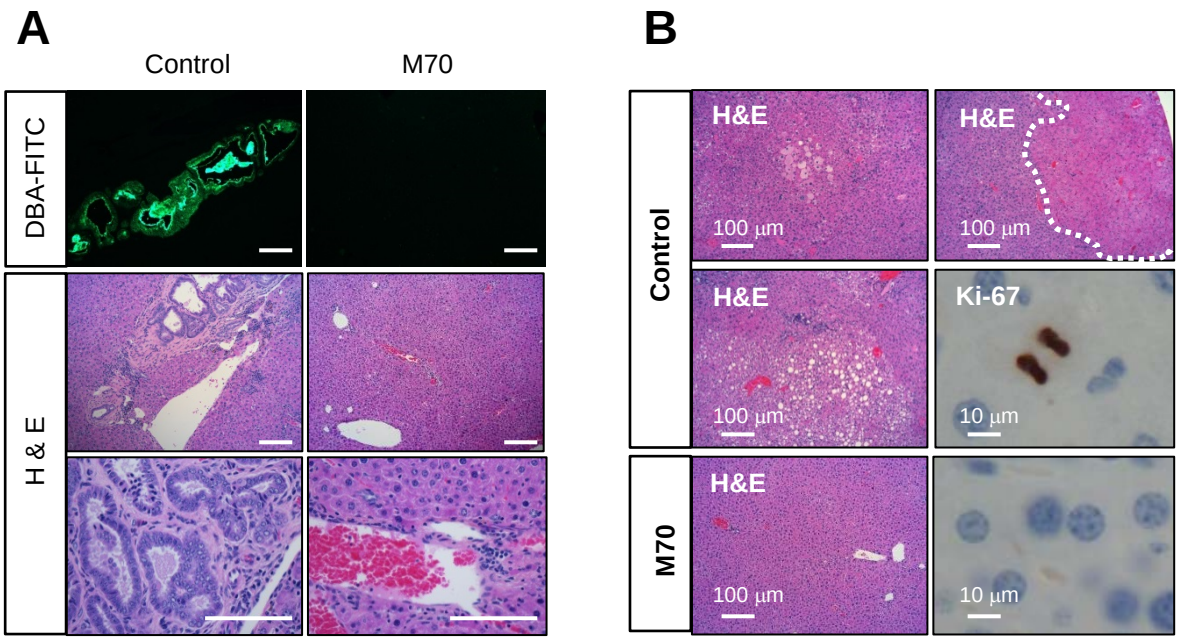

Supplementary Figure 4. Anti-proliferative effects of M70 in *Mdr2-/-* mice. 12-week old *Mdr2-/-* mice received a single dose of AAV carrying M70 or a control (C) gene (*n* = 5 per group). Liver histology was determined 24 weeks after AAV administration. (**A**) Representative images of the bile ducts. Bile ducts were stained with fluorescein (green)-labelled *Dolichos biflorus* agglutinin (DBA) or H&E. The pronounced bile duct proliferation and biliary tract expansion in *Mdr2-/-* mice were reversed by M70 treatment. Scale bars, 100 μm. (**B**) Cytological atypia (top left panel), dysplasia (top right panel, outlined with dashed line), architectural disorganization (middle left panel) and aberrant mitotic figures (middle right panel) are frequently observed in livers from control *Mdr2-/-* mice, but not in M70-treated mice. Scale bars are shown in each panel.